Proc. the First International Symposium on Advanced Fluid Information
Miyagi Zao Royal Hotel, Sendai, Jpaan, Octorber 4-5, 2001

Direct Numerical Simulation of Passive Scalar Transfer Across a Turbulent Gas-Liquid Interface

Yosuke HASEGAWA*, Nobuhide KASAGI*, and Hideshi HANAZAKI**

Direct numerical simulation (DNS) of the coupled air-water turbulent flow has been carried out. The large effect of the interaction between gas and liquid on turbulent structures is observed very close to the interface (y^+<1.0) in the gas phase. The turbulent structures in this region are driven by those of the liquid phase due to the large density difference between the two fluids, although, except for this region, the streaky structures are determined by the physical property in each phase. We applied a Lagrangian method to passive scalar transfer for high Schmidt numbers (Sc = 100, 300, 500 and 1000), respectively, at different Reynolds numbers (Re_τ = 150 and 300) and obtained gas transfer rates which found to be proportional to $Re_\tau^{-1/2} \cdot Sc^{-1/2}$. With increasing the Schmidt number, the fluctuations at low wave numbers play an important role in mass transfer, while the contributions from high wave numbers tend to decrease although a large amount of concentration fluctuations is contained in this region.

1. Introduction

The mass transfer phenomena are important in many engineering, geophysical and environmental problems. Among them, the exchange of slightly soluble gases like O_2 or CO_2 between the atmosphere and the sea surface are of particular interest when considering the global environmental problem. For such gases, the concentration boundary layer in a liquid phase is extremely thin (less than 0.2 mm), while mass transfer is governed by the turbulent structures in the vicinity of the interface.

Direct numerical simulation would be a powerful tool for studying this problem and has been carried out in many previous studies. Lam and Banerjee[1] observed streaky structures, which are similar to the wall-layer streaks, near the free-slip surface under a sufficiently high shear. The average spanwise spacing between the streaks was about 100, when nondimensionalized by the kinematic viscosity and the friction velocity at the interface.

In the case of the real sea surface, the effect of the interaction between gas and liquid turbulent flows would be important, especially for slightly soluble gases. Lombardi *et al.*[2] have carried out DNS of coupled air-water turbulent flow. In their study, the streaky structures coupled with the quasi-streamwise vortices were observed in both gas and liquid phases. However, in those studies, the viscous lengths in the two phases were assumed to be the same, although the real viscous length of the liquid phase is about two times larger than that of the gas phase under the standard conditions (at atmospheric pressure and 293 K). Hence, it is of interest to investigate how the interactions and the associated turbulence structures near the interface are affected by the difference in the viscous lengths between the two fluids.

Although DNS has an advantage of clarifying the complex mechanisms of mass transfer, the computational load would be too large for scalars with high Schmidt numbers, such as O_2 or CO_2 (Sc ~ 600). Recently, however, Na *et al.*[3] have applied a Lagrangian method to passive scalar transfer at high Schmidt numbers in a turbulent channel flow. Their results showed good agreement with the experimental data.

In this study, we have carried out DNS, in which gas and liquid phases are coupled each other without complexity of the interface deformation, to investigate the effect of the different physical properties of air and water. To calculate the mass transfer, we have employed the Eulerian method for low Schmidt numbers (Sc = 1.0 and 3.0) and the Lagrangian method for high Schmidt numbers (Sc = 100, 300, 500 and 1000), respectively, at different Reynolds numbers (Re_τ = 150 and 300).

2. Numerical method

In Fig. 1, the computational domain is shown. The depth of both subdomain is δ, and their horizontal dimensions are $2.5\pi\delta$ and $\pi\delta$ in the streamwise and spanwise directions, respectively. Periodic boundary conditions are imposed in the two horizontal directions. No-shear boundary conditions are applied at the outer edge of each domain. At the interface of two

* Dept. of Mech. Eng., The University of Tokyo, 7-3-1 Hongo, Bunkyo-ku, Tokyo 113-8656, Japan
** Institute of Fluid Science, Tohoku University, 2-1-1 Katahira, Aoba-ku, Sendai, Miyagi 980-8577, Japan

subdomains, the continuities of the velocity, shear stress, scalar concentration and scalar flux are imposed. The effect of free surface deformation is not accounted for, since the effect of deformation on turbulence and mass transfer is negligible in low-Reynolds number turbulence. In this study, pressure fluctuations at the interface are also sufficiently small compared with the atmospheric pressure, so that it is assumed that the Henry's coefficient of gas absorption is constant. The density ratio of the two fluids is $\rho_L/\rho_G = 841$, which roughly corresponds to air and water at the atmospheric pressure and 320 K. The details of the numerical algorithm are essentially the same as Lombardi *et al.*[2]

In this study, simulations are carried out for three different cases (see Table 1). In case 1, the Reynolds numbers ($Re_\tau = u_\tau\delta/\nu$) based on the depth of each domain δ, the friction velocity at the interface u_τ, and the kinematic viscosity ν of each fluid are set to be 150 in both subdomains. In case 2, the Reynolds numbers are increased to 300 in both subdomains. In the present study, the same Reynolds numbers in both gas and liquid phases are equivalent to assuming the same viscous lengths in air and water. However, the real viscous length of the liquid phase is about two times larger than that of the gas phase under the standard conditions. Therefore, in case 3, the Reynolds number is set to be 150 in the liquid phase, while it is 300 in the gas phase.

3. Turbulent structures near the interface

3. 1 Statistics

Figures 2 and 3 show the root-mean-square (rms) velocity fluctuations in the liquid and gas phases normalized by the friction velocity u_τ in each phase. We also plotted those of a turbulent channel flow at Re_τ =150 for comparison. The distribution of u_{rms} in the liquid phase has its maximum at the interface, while in the gas phase, the turbulent intensities have similar trends to those of wall turbulence. This difference between the gas and liquid phases results from the large density ratio between the two fluids, so the interface acts as something like a no-slip wall for the gas, whilst, for the liquid, it is similar to a free-slip boundary. Because the friction velocity u_τ is different in each phase ($u_{\tau G}/u_{\tau L} = 29$), the dimensional intensities are exactly same at the interface in the two fluids.

Table 1 Computational parameters

	Re_τ Gas phase	Re_τ Liquid phase	ρ_L/ρ_G Density ratio	$l_{\tau L}/l_{\tau G}$ Viscous length ratio
Case 1	150	150	841	1.0
Case 2	300	300	841	1.0
Case 3	300	150	841	2.0

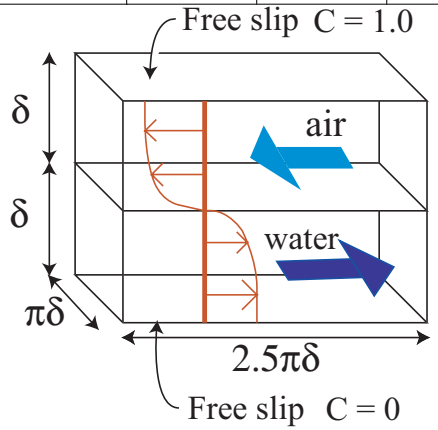

Fig. 1 Computational domain

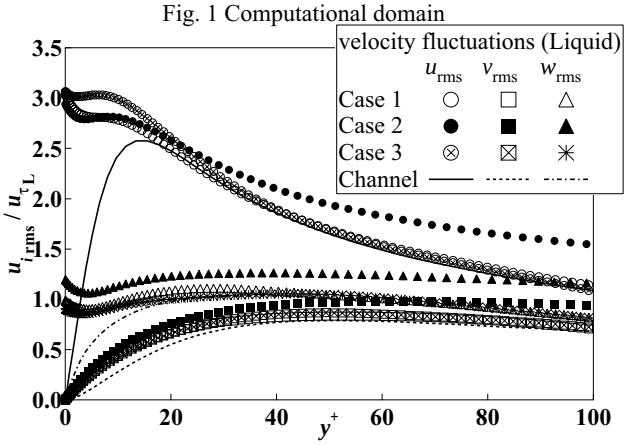

Fig. 2 Velocity fluctuations in the liquid phase

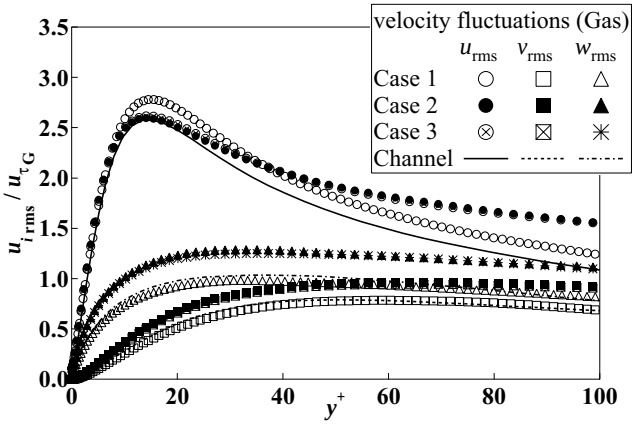

Fig. 3 Velocity fluctuations in the gas phase

With increasing the Reynolds number to Re_τ = 300 (case 2), the vertical and spanwise velocity fluctuations are increased near the interface in both phases, while the streamwise velocity fluctuation is almost kept unchanged (slightly decreased). This change is due to the increase in the pressure strain terms (not shown here).

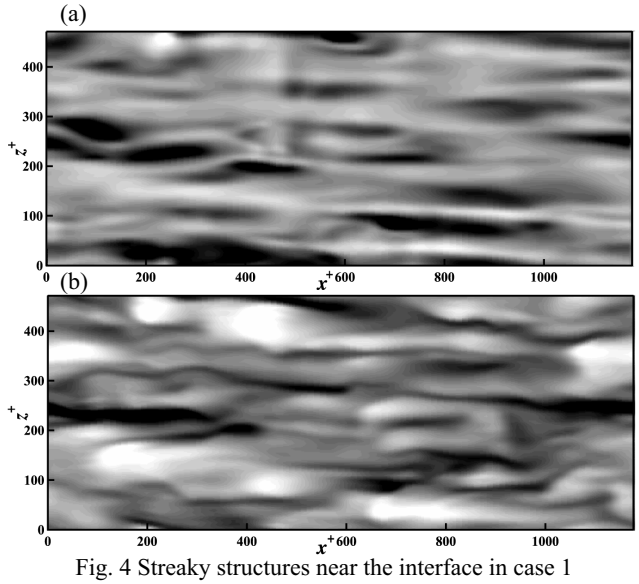

Fig. 4 Streaky structures near the interface in case 1
(a) gas side $y^+ = 1.0$, (b) liquid side $y^+ = 1.0$

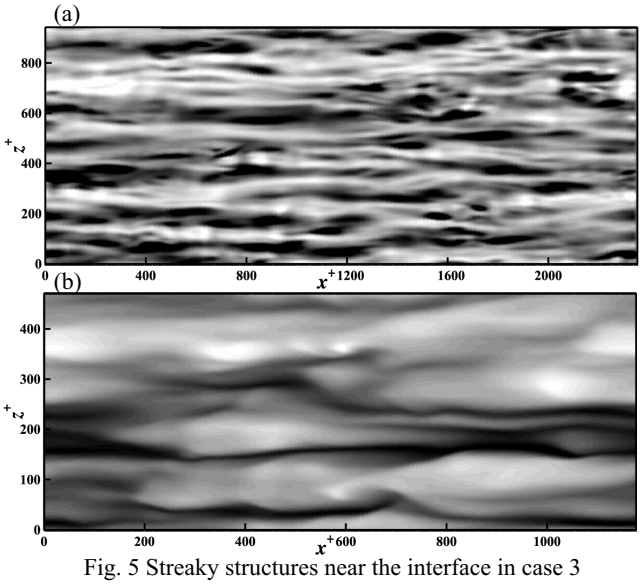

Fig. 5 Streaky structures near the interface in case 3
(a) gas side $y^+ = 1.0$, (b) liquid side $y^+ = 1.0$

3. 2 Effect of viscous lengths

In Figs. 4(a) and (b), the contours of streamwise velocity fluctuations of case 1 near the interface in both phases show similar streaky structures. The average spanwise spacing between the streaks is about 100 shear-based units (l^+_G, $l^+_L \sim 100$) in both phases. In case 2 similar streaky structures are also found, but with much different streak spacings. However, it is again about100 shear-based length on both sides of the interface (not shown here). These results suggests that the average spanwise spacing between the streaks is determined by the viscous length of each phase. In case 3, two times larger viscous length is assumed in the liquid phase, which corresponds to the physical properties of air and water under the standard conditions. In Fig. 5, the contours of streamwise velocity fluctuations at $y^+ = 1$ in both phases are shown. The spacing of streaks in the liquid phase is about two times larger than that in the gas phase. It is very interesting that turbulent structures in each phase are determined by the viscous length of each fluid even very close to the interface ($y^+ = 1$). It is also found that the spacing of streaky structures at the interface is governed by the liquid phase rather than the gas phase (not shown here).

From the above, it is expected that the streaky structures change near the interface on the gas side (less than $y^+ = 1$) and this is actually the case. The correlations between velocities at the interface and different vertical locations (y) in case 3 defined as follows,

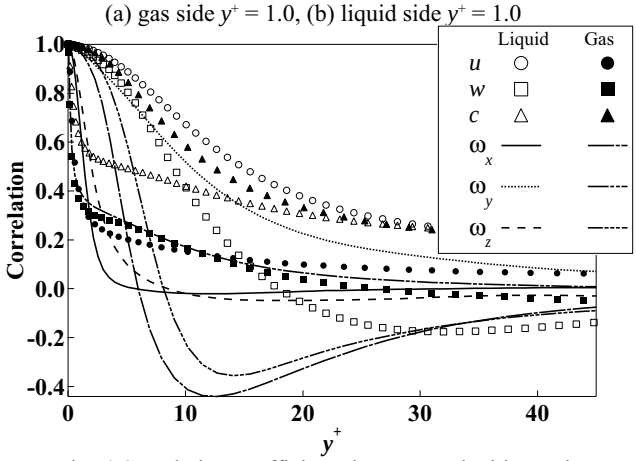

Fig. 6 Correlation coefficients between velocities and scalar at the interface and different vertical locations (y) in case 3 (near the interface)

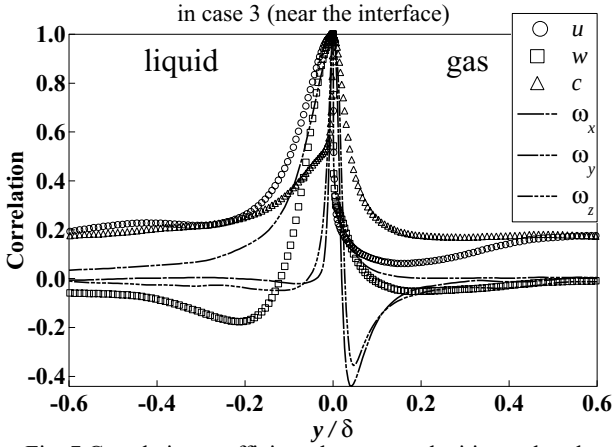

Fig. 7 Correlation coefficients between velocities and scalar at the interface and different vertical locations (y) in case 3

$$C_{u_i}(\Delta y) = \frac{\overline{u_i(x,0,z)\cdot u_i(x,\Delta y,z)}}{u_{i_{rms}}(0)\cdot u_{i_{rms}}(\Delta y)} \qquad (1)$$

are shown in Figs. 6 and 7. The correlation coefficients of u and w in the gas phase are decreased near the interface much more rapidly than that of the liquid phase (Fig. 6).

These results can be explained as follows. Due to the large density ratio between the two fluids, the effect of the shear stress fluctuations at the interface on streaky structures in the liquid phase is negligibly small, on the other hand, the turbulent structures of the gas phase are driven by the streaks of the liquid phase very close to the interface (y^+<1.0). However, except for this region, the streaky structures are determined by the physical property in each phase.

On the contrary, the correlation coefficient of scalar is higher on the gas side, because molecular diffusion from the interface dominates the scalar field rather than turbulent diffusion. The correlation coefficients of ω_y decreases slowly close to the interface in the liquid phase due to surface-connected eddies on the liquid side, and negative peaks of those of ω_x, ω_z are observed near the interface (y^+~15) in the gas phase due to the almost no-slip condition at the interface. It is also found that the correlations of *u* and *w* have non-zero value even far from the interface on the both sides (Fig. 7). It indicates the existence of large scale eddies scaled by δ. This point will be discussed Sec. 4. 4.

4. Mass transfer across the interface for high Schmidt numbers

4.1 Lagrangian method

Computation of the concentration fields for Schmidt numbers as high as those of O_2 or CO_2 by the Eulerian method is unrealistic because the number of grid points increases due to the very thin scalar boundary layers. In this study, the Lagrangian method developed by Papavasilliou *et al.*[4, 5] is employed for high Schmidt numbers (*Sc* = 100, 300, 500 and 1000). In this method, trajectories of scalar markers which move due to convective and molecular effects are calculated in DNS.

4. 2 Classical mass transfer models

To estimate the mass transfer across an interface, simple predictive models are necessary. The surface-renewal model, which was originated by Danckwerts[6], proposes that the exchange of fluids between the surface and the bulk is essential for the mass transfer. In this model, the gas transfer rate *K* is calculated as follows,

$$K = \sqrt{D/\tau}, \qquad (2)$$

where *D* is molecular diffusivity, and τ is the surface renewal time. The main problem in this model is the prediction of τ. Fortescue and Pearson[7] assumed that the large scale eddies scaled by δ dominate mass transfer, and obtained $\tau \propto \delta / u_\tau$, which yields,

$$K^+ = K/u_\tau = C_L \cdot Sc^{-1/2} \cdot Re_\tau^{-1/2}, \qquad (3)$$

where u_τ is the friction velocity at the interface. On the other hand, if one assume that transfer is governed by the smallest scale of eddies, the time scale becomes $\tau \propto (\nu/\varepsilon)^{1/2}$ (the Kolmogorov timescale).[8] Then, one obtains,

$$K^+ = K/u_\tau = C_S \cdot Sc^{-1/2} \cdot Re_\tau^{-1/4}. \qquad (4)$$

To verify those models, varying the Reynolds number Re_τ and observing the dependence of the gas transfer rate on it are desirable. In the following sessions, gas transfer rates at different Reynolds numbers, and the related turbulent structures will be discussed.

4. 3 Mass transfer for high Schmidt numbers

With increasing the Schmidt number in the liquid phase, almost all the resistance to the absorption occurs in the liquid phase, so that we can assume the constant concentration at the interface for high Schmidt numbers, and solve only the liquid side concentration. The detailed discussion is found in Hasegawa and Kasagi[9]. In Fig. 8, the gas transfer rates for high Schmidt numbers at different Reynolds numbers are shown. In both case1 (Re_τ=150) and case 2 (Re_τ=300) , the gas transfer rates are proportional to $Sc^{-0.5}$. These data can be compiled as follows,

$$K^+ = K/u_\tau = \alpha \cdot Sc^{-1/2} \cdot Re_\tau^{-1/2} \qquad (5)$$

with α = 1.8, which is in agreement with equation (3). This suggests that large scale eddies rather than small scale eddies, are responsible for mass transfer at high Schmidt numbers.

In Fig. 9, the limiting behavior of eddy diffusivity for scalar is shown. With the Schmidt number increased, the concentration boundary layer becomes very thin (y^+ < 1.0). Furthermore, from the fact that the gas transfer rates are proportional to $Re_\tau^{-0.5}$, it is derived that the eddy diffusivity is proportional to $Re_\tau^{-1} \bullet y^{+2}$ near the interface, as follows,

$$Ec = \beta \cdot Re_\tau^{-1} \cdot y^{+2} \qquad (5)$$

where β is about 9.0. This face is confirmed in Fig. 9.

4. 4 Correlations between scalar and velocity fields near the interface

Two point correlation function between fluctuations of surface scalar flux and velocity fields at a low Schmidt number (Sc = 1.0 in both phases) in the y-z plane were calculated from the Eulerian data. The two point correlation $C_{v_i}(\Delta x, \Delta y, \Delta z)$ is defined as follows:

$$C_{v_i}(\Delta x, \Delta y, \Delta z) = \frac{\overline{q'(x,z)|_{\text{surface}} \cdot v_i'(x+\Delta x, y+\Delta y, z+\Delta z)}}{q_{\text{rms}}|_{\text{surface}} \cdot v_{i\,\text{rms}}(y+\Delta y)} \quad (7)$$

where $q' = -D \cdot \partial c' / \partial y$ is the fluctuating part of the surface scalar flux. The horizontal center line in Fig. 10 stands for the interface and gradation represents the correlation of the scalar field (positive denoted by black, negative by white). It is found that the quasi-streamwise vortices near the interface in the liquid phase contribute to the surface scalar flux more than those in the gas phase. This is because the limiting value of the normal velocity fluctuation in the liquid is much larger than that in the gas phase due to the effect of the density ratio between the two fluids.

In addition, large scale eddies scaled by δ and associated scalar fluctuations are found in both phases. Therefore, not only the quasi-streamwise vortices near the interface, but also the large scale vortices scaled by δ govern the surface scalar flux at a low Schmidt number.

4. 5 Wavenumber spectra for concentration fluctuations

In Fig. 11, the spectral density functions of u, v and c at different Schmidt numbers (Sc = 1.0, 3.0) versus wavenumber in the spanwise direction, kz , near the interface (y^+ = 1.0) in the liquid phase, are shown. The peak of v' at $kz \sim 5$ corresponds to the quasi-streamwise vortices, while the large eddies scaled by δ corresponds to $kz \sim 2$. With increasing the Schmidt number, the contribution of high wave numbers to the scalar fluctuation increases. However, it is interesting that in Fig. 12, the co-spectral density functions for $\overline{c'v'}$ are almost kept unchanged. It is also found that the contributions of the quasi-streamwise vortices ($kz \sim 5$) and the larger scale vortices are slightly increased at a higher Schmidt number (Sc = 3.0), although the contribution of high wave numbers ($kz > 10$) decreases. This is because the correlation of the normal velocity

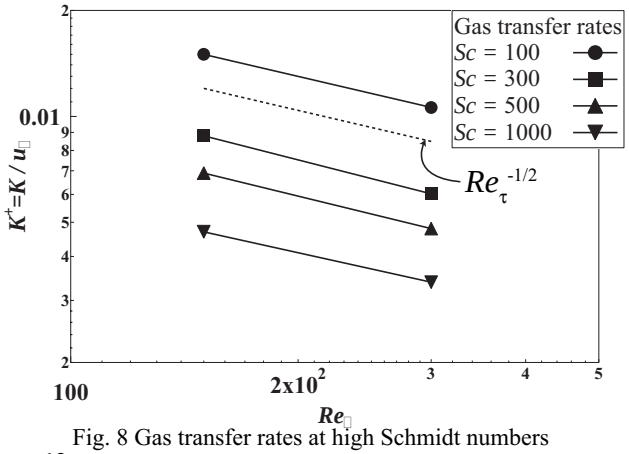

Fig. 8 Gas transfer rates at high Schmidt numbers

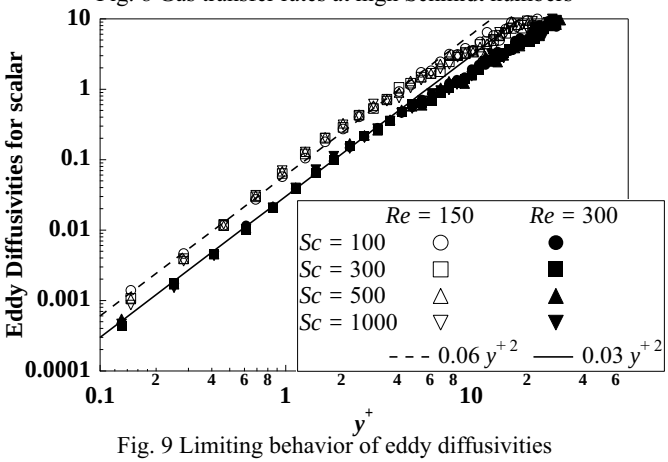

Fig. 9 Limiting behavior of eddy diffusivities near the air-water interface

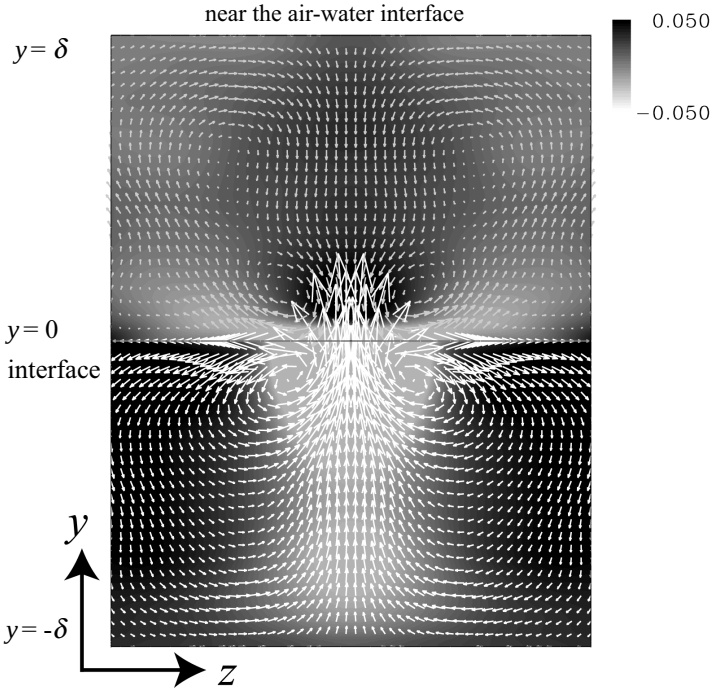

Fig. 10 Correlation functions between the surface scalar flux and velocity and scalar fields

(v') and the scalar concentration (c') is strongly dumped at higher wave numbers ($kz > 10$) as shown in Fig. 13.

From these results, it is expected that only the low wavenumbers play an important roll in mass trans-

fer for high Schmidt numbers and the contributions from higher wave numbers tend to decrease, although a large portion of scalar fluctuations is contained in this region. This phenomenon is also found in wall turbulence.(3)

5. Conclusions

Direct numerical simulation of the coupled gas-liquid turbulent flow was carried out. Varying the viscous lengths in both phases, the large effects of the interaction between two fluids are observed in the vicinity of the interface (y^+<1.0) on the gas side due to the large density ratio of the two fluids.

Employing the Lagrangian method, the gas transfer rates at high Schmidt numbers were calculated and found to be almost proportional to $Re_\tau^{-0.5} \cdot Sc^{-0.5}$. In this study, it is confirmed that the two kinds of eddies, *i.e.,* the quasi-streamwise eddies near the interface and the large eddies scaled by δ, contribute to the scalar flux at the interface at a low Schmidt number. It is expected that the smallest scale eddies would not contribute to mass transfer, because the correlation of v and c at high wave numbers are decreased rapidly at high Schmidt numbers. However, in this study, it was not obvious which structure (the quasi-streamwise eddies near the interface or large eddies scaled by δ) governs mass transfer at sufficiently high Schmidt numbers. The Eulerian calculations at higher Schmidt numbers would be required to clarify this problem.

6. References

(1) Lam, K., and Banerjee, S., On the Condition of Streak Formation in a Bounded Turbulent Flow., Phys. Fluids., A4 (1992), p. 306-320.
(2) Lombardi, P., De Angelis, V., and Banerjee, S., Direct Numerical Simulation of near-interface turbulence in coupled gas-liquid flow., Phys. Fluids., Vol. 11., No. 6 (1996), p. 2607-2625.
(3) Na. Y., Papavassiliou, D., and Hanratty T. J., Use of direct numerical simulation to study the effect of Prandtl number on temperature fields., Int. J. Heat and Mass Transfer., Vol. 20 (1999), p. 187-195.
(4) Papavassiliou, D. V., and Hanratty T. J., The Use of Lagrangian Methods to Describe Turbulent Transport of Heat from a Wall., Ind. Eng. Chem. Res., Vol. 34 (1995), p. 3359-3367.
(5) Papavassiliou, D. V., and Hanratty T. J., Transport of a Passive Scalar in a Turbulent Channel Flow., Int. J. Heat and Mass Transfer., Vol. 40, No.6 (1997), p. 1303-1311.
(6) Danckwerts, P. V., Significance of Liquid-Film Coefficients in Gas Absorption., Ind. Eng. Chem., Vol. 43 (1951), p. 1460-1467.

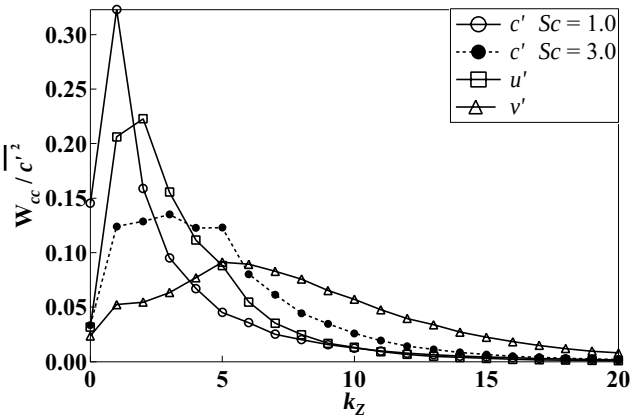

Fig. 11 The spectral dencity functions of u', v' and c' as a function of spanwise wave number k_z

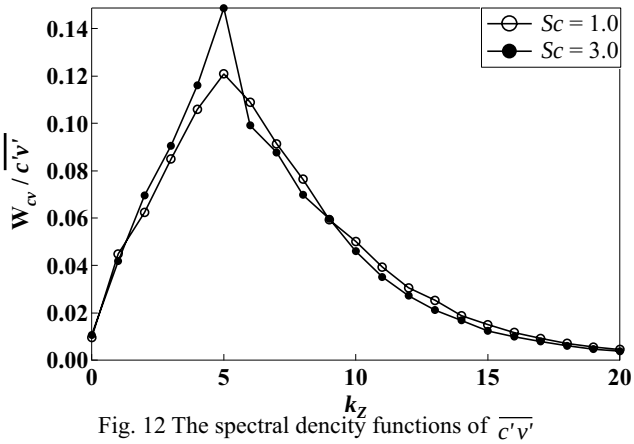

Fig. 12 The spectral dencity functions of $\overline{c'v'}$ as a function of spanwise wave number k_z

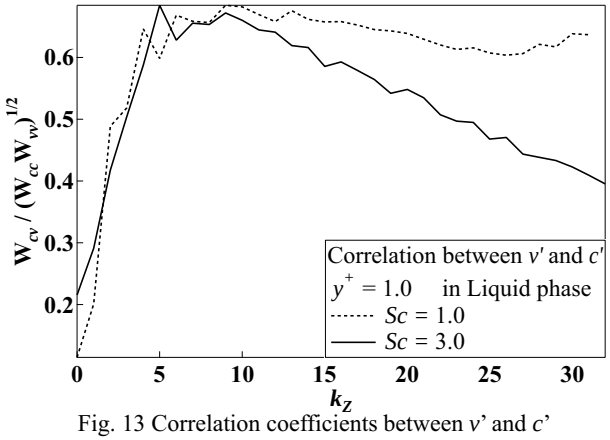

Fig. 13 Correlation coefficients between v' and c' as a function of spanwise wave number k_z

(7) Fortescue, G. E., and Pearson, J. R. A., On Gas Absorption into a Turbulent Liquid., Chem. Eng. Sci. Vol. 22 (1967), p. 1163-1176.
(8) Lamont, J. C., and Scotto, D. S., An Eddy Cell Model of Mass Transfer into the Surface of a Turbulent Liquid., AIChE J., Vol. 16 (1970), p. 513-519.
(9) Hasegawa Y., and Kasagi. N., The Effect of Schmidt Number on Air-Water Interface Mass Transfer., Proc. 4th. Int. Conf. Multiphase Flow., New Orleans, in CD-ROM.
(10) Hanratty, T. J., Effect of Gas Flow on Physical Absorption., Air-Water Gas Transfer, ASCE, New York.
(11) Calmet, I., and Magnaudet J., High-Schmidt Number Mass Transfer Through Turbulent Gas-Liquid Interface., Int. J. Heat and Fluid Flow., Vol. 19 (1998), p. 522-532.